



## Exact analytical solution of unsteady axi-symmetric conductive heat transfer in cylindrical orthotropic composite laminates

A. Amiri Delouei\*, M. H. Kayhani, M. Norouzi

Mechanical Engineering Department, Shahrood University of Technology, Shahrood, Iran

### ARTICLE INFO

#### Article history:

Received 4 November 2011

Received in revised form 16 March 2012

Accepted 19 March 2012

Available online 8 May 2012

#### Keywords:

Analytical solution

Cylindrical composite laminate

Unsteady heat conduction

Laplace transformation

Meromorphic function method

### ABSTRACT

This study presents an exact analytical solution of transient heat conduction in cylindrical multilayer composite laminates. This solution is valid for the most generalized linear boundary conditions consisting of the conduction, convection and radiation heat transfer. Here, it is supposed that the fibers are wound around the cylinder and their direction can be changed in each lamina. Laplace transformation is applied to change the domain of the solutions from time into the frequency. An appropriate Fourier transformation has been derived using the Sturm–Liouville theorem. Here, a set of equations for Fourier coefficients are obtained based on the boundary conditions both inside and outside the cylinder, and the continuity of temperature and heat flux at boundaries between adjacent layers. The exact solution of this set of equations is obtained using Thomas algorithm and Fourier coefficients are expressed by recessive relations. Due to the difficulty of applying the inverse Laplace transformation, the Meromorphic function method is utilized to find the transient temperature distribution in laminate. Some industrial examples are presented to investigate the ability of current solution for solving the wide range of applied steady and unsteady problems.

© 2012 Elsevier Ltd. All rights reserved.

### 1. Introduction

Current developments in composite materials have introduced these materials as the best choice in many branches of engineering applications. This is generally related to some advantages of these materials such as higher ratio of strength to weight, plasticity, low cost and their unique behavior of anti-corrosion. Today, composite materials have been used abundantly in different fields of industrial applications such as aerospace [1–3], brake and friction systems [4,5], fins, vessels, heat exchangers [6–9], electrical application [10,11] and biomaterials [12,13]. Although, there are a lot of articles that deal with mechanical and thermo-mechanical behaviors of these materials, [14–17] just a few studies related to heat conduction phenomena are available. It is important to mention that heat conduction is very significant in manufacturing process [18–20], thermal fraction analysis [21–23] and on the like.

Previous investigations of the heat transfer in composite materials have been restricted mostly to numerical analysis. A new approximated computational model has been proposed by Blanc and Touratier [24] to analyze heat transfer in composite materials. In fact, this approach is completely coincident with a finite element approximation in one-dimensional problems. A computational

study of heat transfer in unidirectional composites using homogenization technique and finite element method is presented by Kaminski [25]. He showed that the real composite behavior is estimated by the homogenized model response. Corlay and Advani [26] worked on the determination of numerical and experimental temperature of a thin composite plate that is subjected to a concentrated heat source. They conducted a parametric investigation to determine impressive dimensionless numbers and their effect on the temperature distribution. A numerical model for thermal conductivities of four-axial non-woven composites (NWCs) has been proposed using thermal resistance concept by Lee et al. [27]. It has been shown that when the NWCs are reinforced with rods of the same diameters in in-plane directions, they can possess transverse isotropy. Similar works have been done for heat transfer through woven textiles [28,29].

A number of analytical investigations have been performed in this discipline. Ma et al. [30,31] have developed an analytical solution of heat conduction problem for an anisotropic medium; they used a linear transformation to convert the original anisotropic problem to an equivalent isotropic problem with a same geometrical configuration. Analytical two-dimensional heat conduction in polar coordinate for a multi-layer medium has been presented by Singh et al. [32]; separation of variables method has been used to achieve the transient temperature distribution which is only valid for homogenous boundary conditions of the first and second kind in the angular direction. Kayhani et al. [33] presented an exact

\* Corresponding author.

E-mail addresses: [a.a.delouei@gmail.com](mailto:a.a.delouei@gmail.com) (A. Amiri Delouei), [h\\_kayhani@shahroodut.ac.ir](mailto:h_kayhani@shahroodut.ac.ir) (M. H. Kayhani), [mnorouzi@shahroodut.ac.ir](mailto:mnorouzi@shahroodut.ac.ir) (M. Norouzi).

solution for steady state conductive heat transfer of cylindrical composite laminates in radial and angular directions just available for geometries with a high ratio of longitudinal to radial dimension. An analytical solution for heat conduction of cylindrical composite laminate in longitudinal and radial directions has been also done by Kayhani et al. [34]. They obtained a closed form of temperature distribution for steady state condition.

In the present paper, unsteady heat conduction in composite laminates has been investigated analytically. Laminate is in cylindrical shape and the fibers are wound around the cylinder. The direction of fibers could be varied layer by layer. Fig. 1 shows the geometry of such composite cylinder. Axisymmetric unsteady heat transfer in longitudinal and radial directions ( $r, z$ ) has been focused in this research. Unlike the work of Kayhani et al. [34] which expressed a solution for steady state condition, the current paper presents an analytical solution for transient conductive heat transfer in cylindrical multi-layer composite laminates as a more generalized solution. Here, the authors considered the most general linear boundary conditions. Using this solution, it is possible to investigate the combined effects of conduction, convection and radiation both inside and outside the cylindrical composite laminates which is the main innovation of current study. The Laplace transformation has been used to change the problem domain from time into frequency. The resulted partial differential equation has been simplified into an ordinary differential equation by applying an appropriate Fourier transformation. This Fourier transformation has been derived using the Sturm–Liouville theorem. Here, a set of equations for Fourier coefficients are obtained based on the boundary conditions both inside and outside the cylinder and temperature/heat flux continuity at boundaries located between the layers. The exact solution of this set of equations is obtained using Thomas algorithm and Fourier coefficients are expressed by recessive relations. Finally, the inverse Fourier and inverse Laplace transformations have been respectively applied, to attain the time dependent temperature distribution of composite laminate. The main problem encountered at this stage is the difficulty to solve the complex integral of inverse Laplace. Here, the authors use a technique called “Meromorphic function method” to overcome on this problem. This general solution has been utilized on some applied examples to verify the ability of the current solution in achieving the transient temperature distribution in different industrial situations.

**2. Conductive heat transfer in composites**

In this section, the basic concepts of conductive heat transfer in composite laminates are presented briefly. Fourier law for conductive

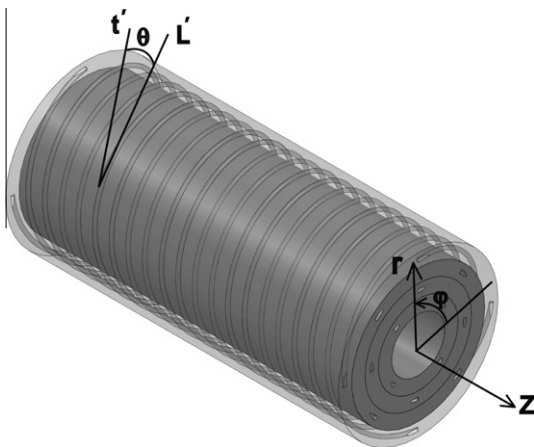


Fig. 1. Direction of fibers in a cylindrical laminate.

heat transfer in orthotropic mediums in a cylindrical system is as follows [35]:

$$\begin{Bmatrix} q_r \\ q_\phi \\ q_z \end{Bmatrix} = - \begin{bmatrix} k_{11} & k_{12} & k_{13} \\ k_{21} & k_{22} & k_{23} \\ k_{31} & k_{32} & k_{33} \end{bmatrix} \begin{Bmatrix} \frac{\partial T}{\partial r} \\ \frac{1}{r} \frac{\partial T}{\partial \phi} \\ \frac{\partial T}{\partial z} \end{Bmatrix} \tag{1}$$

where  $q$  is heat flux,  $k_{ij}$  is conductive heat transfer coefficient and  $T$  is temperature. The relations between heat conduction coefficients has been investigated in details by Fung [36] and Powers [37]. In order to study the heat conduction in composite laminates, two different coordinate systems should be defined [38]. Here,  $(x_1, x_2, x_3)$  and  $(r, \phi, z)$  are considered as on-axis and off-axis coordinate systems, respectively. Off-axis coordinate system is defined to study the thermal properties in unique directions. The direction of on-axis coordinates depends on fiber orientation, in a way that  $x_1$  is indirection of the fibers,  $x_2$  is perpendicular to the fiber direction located in the plane of lamina and  $x_3$  is the third orthogonal direction. The fiber direction in each layer can be different from the other layers. Therefore, on-axis and off-axis systems have an angular deviation equal to  $\theta$  in each lamina. The Fourier law in on-axis coordinate system can be written as [39]:

$$\begin{Bmatrix} q_r \\ q_\phi \\ q_z \end{Bmatrix} = - \begin{bmatrix} k_{22} & 0 & 0 \\ 0 & k_{11} & 0 \\ 0 & 0 & k_{22} \end{bmatrix}_{on} \begin{Bmatrix} \frac{\partial T}{\partial r} \\ \frac{1}{r} \frac{\partial T}{\partial \phi} \\ \frac{\partial T}{\partial z} \end{Bmatrix} \tag{2}$$

In this study, the composite laminate is in cylindrical shape. Hence, the problem must be solved in a cylindrical coordinate system. As shown in Fig. 1, the fibers have been wound in specific directions around the cylinder. Here,  $\theta$  is the angle between the tangent line on cylinder in  $\phi$  direction ( $t'$ ) and the tangent line in fibers' direction ( $L'$ ). Applying the rotation  $\theta$  to the on-axis conductivity tensor  $[k]$ , the off-axis conductivity tensor  $[\bar{k}]$  is obtained [34]:

$$\begin{aligned} \bar{k}_{11} &= k_{22} \\ \bar{k}_{22} &= m_i^2 k_{11} + n_i^2 k_{22} \\ \bar{k}_{33} &= n_i^2 k_{11} + m_i^2 k_{22} \\ \bar{k}_{12} &= \bar{k}_{21} = 0 \\ \bar{k}_{13} &= \bar{k}_{31} = 0 \\ \bar{k}_{23} &= \bar{k}_{32} = m_i n_i (k_{11} - k_{22}) \end{aligned} \tag{3}$$

In these relations,  $m_i$  and  $n_i$  represent  $\cos \theta$  and  $\sin \theta$ , respectively. Using the balance of energy in a cylindrical element and substituting Eq. (3) into the Eq. (1), the two-dimensional unsteady heat conduction equation in cylindrical laminate will be achieved:

$$\begin{aligned} k_{22} \frac{1}{r} \frac{\partial}{\partial r} \left( r \frac{\partial T}{\partial r} \right) + (m_i^2 k_{11} + n_i^2 k_{22}) \frac{1}{r^2} \frac{\partial^2 T}{\partial \phi^2} + (n_i^2 k_{11} + m_i^2 k_{22}) \\ \times \frac{\partial^2 T}{\partial z^2} + 2m_i n_i (k_{11} - k_{22}) \frac{1}{r} \frac{\partial^2 T}{\partial \phi \partial z} \\ = \rho c_p \frac{\partial T}{\partial t} \end{aligned} \tag{4}$$

where  $\rho$  and  $c_p$  are density and specific heat capacity at constant pressure, respectively. Due to the multi-layer form of laminate, it is necessary to obtain the relation between the temperature and heat flux of layers. Fig. 2 shows the arrangement of the layers in the cylindrical laminate. If  $r = r_i$  is boundary between two layers  $i$  and  $i + 1$ , then temperature continuity and heat flux continuity will be as follows:

$$T^{(i)} = T^{(i+1)} \tag{5a}$$

$$k_{22}^{(i)} \frac{\partial T^{(i)}}{\partial r} = k_{22}^{(i+1)} \frac{\partial T^{(i+1)}}{\partial r} \tag{5b}$$

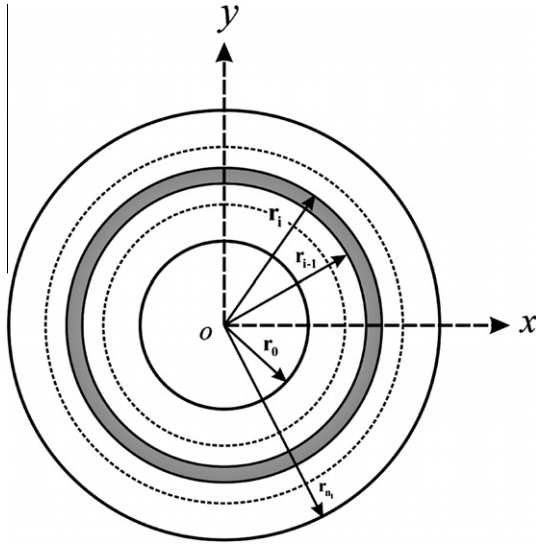


Fig. 2. Arrangement of layers in a cylindrical laminate.

3. Analytical solution

In this section, the analytical solution of unsteady temperature distribution under generalized linear boundary conditions is presented. For simplification, the modified temperature has been defined as:

$$\phi(r, z, t) = T(r, z, t) - T_i \tag{6}$$

where  $T_i$  is the initial temperature of laminate. The energy equation for two-dimensional heat conduction in radial and longitudinal directions can be written as:

$$\alpha_r \frac{\partial^2 \phi}{\partial r^2} + \alpha_r \frac{1}{r} \frac{\partial \phi}{\partial r} + \alpha_{z,i} \frac{\partial^2 \phi}{\partial z^2} = \frac{\partial \phi}{\partial t} \tag{7}$$

where

$$\alpha_r = \frac{k_{22}}{\rho c_p} \tag{8a}$$

$$\alpha_{z,i} = \frac{n_i^2 k_{11} + m_i^2 k_{22}}{\rho c_p} \tag{8b}$$

It is important to mention that  $\alpha_{z,i}$  is a function of fibers' angle in each layer and can be changed layer by layer. Initial condition and general linear boundary conditions can be expressed as follows:

$$\phi^{(i)}(r, z, 0) = 0, \quad i = 1, 2, \dots, n_i \tag{9a}$$

$$a_1 \phi(r, 0, t) + b_1 \frac{\partial \phi(r, 0, t)}{\partial z} = f_1(r, t) \tag{9b}$$

$$a_2 \phi(r, L, t) + b_2 \frac{\partial \phi(r, L, t)}{\partial z} = f_2(r, t) \tag{9c}$$

$$c_1 \phi(r_0, z, t) + d_1 \frac{\partial \phi(r_0, z, t)}{\partial r} = g_1(z, t) \tag{9d}$$

$$c_2 \phi(r_{n_i}, z, t) + d_2 \frac{\partial \phi(r_{n_i}, z, t)}{\partial r} = g_2(z, t) \tag{9e}$$

where  $f_1(r, t)$ ,  $f_2(r, t)$ ,  $g_1(z, t)$ , and  $g_2(z, t)$  are arbitrary functions. The constant coefficients  $a_1$ ,  $a_2$ ,  $c_1$ , and  $c_2$  have the same dimensions as the convection coefficient (i.e.,  $W/m^2 K$ ), whereas  $b_1$ ,  $b_2$ ,  $d_1$ , and  $d_2$  have the same dimensions as the conduction coefficient (i.e.,  $W/m K$ ). Laplace transformation has been used to convert the heat

conduction equation (Eq. (7)) from time domain ( $t$ ) into frequency domain ( $s$ ) [40]:

$$L\{\phi(r, z, t)\} = \bar{\phi}(r, z, s) \tag{10}$$

Applying the Laplace transformation and initial condition on Eq. (7), the energy equation in frequency domain is obtained:

$$\alpha_r \frac{\partial^2 \bar{\phi}}{\partial r^2} + \alpha_r \frac{1}{r} \frac{\partial \bar{\phi}}{\partial r} + \alpha_{z,i} \frac{\partial^2 \bar{\phi}}{\partial z^2} - s \bar{\phi} = 0 \tag{11}$$

Furthermore, the boundary conditions in frequency domain can be expressed as:

$$a_1 \bar{\phi}(r, 0, s) + b_1 \frac{\partial \bar{\phi}(r, 0, s)}{\partial z} = \bar{f}_1(r, s) \tag{12a}$$

$$a_2 \bar{\phi}(r, L, s) + b_2 \frac{\partial \bar{\phi}(r, L, s)}{\partial z} = \bar{f}_2(r, s) \tag{12b}$$

$$c_1 \bar{\phi}(r_0, z, s) + d_1 \frac{\partial \bar{\phi}(r_0, z, s)}{\partial r} = \bar{g}_1(z, s) \tag{12c}$$

$$c_2 \bar{\phi}(r_{n_i}, z, s) + d_2 \frac{\partial \bar{\phi}(r_{n_i}, z, s)}{\partial r} = \bar{g}_2(z, s) \tag{12d}$$

where

$$\bar{f}_1(r, z, s) = L\{f_1(r, z, t)\} \tag{13a}$$

$$\bar{f}_2(r, z, s) = L\{f_2(r, z, t)\} \tag{13b}$$

$$\bar{g}_1(r, z, s) = L\{g_1(r, z, t)\} \tag{13c}$$

$$\bar{g}_2(r, z, s) = L\{g_2(r, z, t)\} \tag{13d}$$

Due to the complicated boundary conditions, an appropriate Fourier transformation has been derived using Sturm–Liouville theorem. The Fourier transformation of arbitrary function  $f(z)$  could be written as follows [40]:

$$F(f) = \frac{\int_a^b s(z) f(z) \varphi'_n(z) dz}{\int_a^b s(z) \varphi_n^2(z) dz} \tag{14}$$

where  $s(z)$  is the weighting function and  $\varphi'_n(z)$  is the eigenfunction related to homogenous form of heat transfer equation and boundary conditions in  $z$  direction. In addition, the inverse Fourier transformation has been defined as:

$$f(z) = \sum_{n=0}^{\infty} F(f) \varphi'_n(z) \tag{15}$$

Since we study the unsteady heat conduction in radial and longitudinal direction, the temperature distribution could be separated as two independent functions  $R(r)$  and  $Z(z)$ :

$$\bar{\phi}(r, z, s) = R(r) \cdot Z(z) \tag{16}$$

Substituting Eq. (16) into the Eq. (11), heat conduction equation has been separated as:

$$\alpha^* \frac{R''}{R} + \alpha^* \frac{R'}{R} - s = -\frac{\ddot{Z}}{Z} = \lambda^2 \tag{17}$$

where  $\lambda$  is a constant and  $\alpha^*$  is defined as:

$$\alpha^* = \frac{\alpha_r}{\alpha_{z,i}} \tag{18}$$

The following equation could be found from the Eq. (17):

$$\frac{\partial^2 Z(z)}{\partial z^2} + \lambda^2 Z(z) = 0 \tag{19}$$

Also, homogenous boundary conditions in z direction are:

$$a_1 Z(0) + b_1 \frac{\partial Z(0)}{\partial z} = 0 \tag{20a}$$

$$a_2 Z(L) + b_2 \frac{\partial Z(L)}{\partial z} = 0 \tag{20b}$$

Solving Eq. (19) under the homogeneous boundary conditions (Eq. (20)), the eigenfunction of this problem ( $\varphi'_n$ ) will be achieved:

$$\varphi'_n = (a_1 \sin(\lambda_n z) - b_1 \lambda_n \cos(\lambda_n z)) \tag{21}$$

Eigenvalues ( $\lambda_n$ ) of the Eq. (21) are obtained by solving the following trigonometric equation:

$$(a_1 b_2 - a_2 b_1) \lambda_n \cos(\lambda_n L) + (a_2 a_1 + b_1 b_2 \lambda_n^2) \sin(\lambda_n L) = 0 \tag{22}$$

In this problem, the weighting function ( $S(z)$ ) is constant [40]. Substituting these relations into the Sturm–Liouville Eq. (14), suitable Fourier transformation ( $F$ ) will be obtained:

$$F(f) = \frac{4\lambda_n}{A_n^2} \int_0^L [f(z)(a_1 \sin(\lambda_n z) - b_1 \lambda_n \cos(\lambda_n z))] dz \tag{23}$$

where

$$A_n = \sqrt{(-a_1^2 + (b_1 \lambda_n)^2) \sin(2\lambda_n L) + 2a_1 b_1 \lambda_n \cos(2\lambda_n L) + 2\lambda_n (a_1^2 + (b_1 \lambda_n)^2)L - 2a_1 b_1 \lambda_n} \tag{24}$$

The second order derivation of Fourier transformation is obtained using the fractional integration technique:

$$F(f'') = \left\{ \begin{array}{l} \left(\frac{2\lambda_n}{A_n}\right)^2 \left[ \frac{-a_1}{(a_2 \cos(\lambda_n L) - b_2 \lambda_n \sin(\lambda_n L))} \bar{f}_2(r, s) + \bar{f}_1(r, s) \right] \\ -\lambda_n^2 F(f) \end{array} \right\} \tag{25}$$

Eq. (11) is a second order partial differential equation. By applying the Fourier transformation (Eqs. (23) and (25)) on Eq. (11), the heat conduction will be changed to an ordinary differential equation:

$$\begin{aligned} \alpha^* \frac{\partial^2 U}{\partial r^2} + \alpha^* \frac{1}{r} \frac{\partial U}{\partial r} - (\lambda_n^2 + S/\alpha_{z,i}) U \\ = \left(\frac{2\lambda_n}{A_n}\right)^2 \\ \times \left[ \frac{a_1}{(a_2 \cos(\lambda_n L) - b_2 \lambda_n \sin(\lambda_n L))} \bar{f}_2(r, s) - \bar{f}_1(r, s) \right] \end{aligned} \tag{26}$$

Moreover, boundary conditions in r direction – Eqs. (12c) and (12d) – will be altered:

$$c_1 U(r_0, n, s) + d_1 \frac{\partial U(r_0, n, s)}{\partial r} = G_1(n, s) \tag{27a}$$

$$c_2 U(r_{n_i}, n, s) + d_2 \frac{\partial U(r_{n_i}, n, s)}{\partial r} = G_2(n, s) \tag{27b}$$

where

$$U(r, n, s) = F(\bar{\phi}(r, z, s)) \tag{28a}$$

$$G_1(n, s) = F(\bar{g}_1(z, s)) \tag{28b}$$

$$G_2(n, s) = F(\bar{g}_2(z, s)) \tag{28c}$$

The solution of Eq. (26) is as follows:

$$U^{(i)}(r, n, s) = a_n^{(i)} I_0(\omega_{n,s} r) + b_n^{(i)} K_0(\omega_{n,s} r) + w^{(i)}(r, n, s) \tag{29}$$

where

$$\omega_{n,s,i} = \sqrt{\lambda_n^2 + s/\alpha_{z,i}} \tag{30}$$

and  $w^{(i)}(r, n, s)$  is non-homogenous solution of Eq. (26) and in general form has been written as:

$$\begin{aligned} w^{(i)}(r, n, s) = I_0(\omega_{n,s,i} r) \times \int_{r_0}^{r_{n_i}} [r \times K_0(\omega_{n,s,i} r) \times h(r, n, s)] dr \\ + K_0(\omega_{n,s,i} r) \times \int_{r_0}^{r_{n_i}} [r \times I_0(\omega_{n,s,i} r) \times h(r, n, s)] dr \end{aligned} \tag{31}$$

where

$$h(r, n, s) = \frac{a_1}{(a_2 \cos(\lambda_n L) - b_2 \lambda_n \sin(\lambda_n L))} \bar{f}_2(r, s) - \bar{f}_1(r, s) \tag{31a}$$

$I_0$  and  $K_0$  represent modified Bessel functions of the first and the second kind of order zero, respectively. Regarding to the boundary conditions in r direction and considering the temperature and heat flux continuity at the boundaries located between layers, series coefficients ( $a_n$  and  $b_n$ ) will be achieved:

- Applying boundary condition inside of cylinder (Eq. (27a)):

$$\begin{aligned} a_{n,s}^{(1)} [c_1 I_0(\omega_{n,s,1} r_0) + d_1 \omega_{n,s,1} I_1(\omega_{n,s,1} r_0)] \\ + b_{n,s}^{(1)} [c_1 K_0(\omega_{n,s,1} r_0) - d_1 \omega_{n,s,1} K_1(\omega_{n,s,1} r_0)] \\ = G_1(n, s) - c_1 w^{(1)}(r_0, n, s) - d_1 \frac{\partial w^{(1)}(r_0, n, s)}{\partial r} \end{aligned} \tag{32a}$$

- Applying boundary condition outside of cylinder (Eq. (27b)):

$$\begin{aligned} a_{n,s}^{(n_i)} [c_2 I_0(\omega_{n,s,n_i} r_{n_i}) + d_2 \omega_{n,s,n_i} I_1(\omega_{n,s,n_i} r_{n_i})] \\ + b_{n,s}^{(n_i)} [c_2 K_0(\omega_{n,s,n_i} r_{n_i}) - d_2 \omega_{n,s,n_i} K_1(\omega_{n,s,n_i} r_{n_i})] \\ = G_2(n, s) - c_2 w^{(n_i)}(r_{n_i}, n, s) - d_2 \frac{\partial w^{(n_i)}(r_{n_i}, n, s)}{\partial r} \end{aligned} \tag{32b}$$

- Applying temperature continuity at the boundary located between the layer i and i + 1 (Eq. (5a)):

$$\begin{aligned} U^{(i)}(r_i, n, s) = U^{(i+1)}(r_i, n, s) \\ \Rightarrow a_{n,s}^{(i)} I_0(\omega_{n,s,i} r_i) + b_{n,s}^{(i)} K_0(\omega_{n,s,i} r_i) \\ - a_{n,s}^{(i+1)} I_0(\omega_{n,s,i+1} r_i) + b_{n,s}^{(i+1)} K_0(\omega_{n,s,i+1} r_i) \\ = w^{(i+1)}(r_i, n, s) - w^{(i)}(r_i, n, s) \end{aligned} \tag{32c}$$

- Applying heat flux continuity at the boundary located between the layer i and i + 1 (Eq. (5b)):

$$\begin{aligned} \frac{\partial U^{(i)}(r_i, n, s)}{\partial r} = \frac{\partial U^{(i+1)}(r_i, n, s)}{\partial r} \Rightarrow k_{22}^{(i)} [a_{n,s}^{(i)} \omega_{n,s,i} I_1(\omega_{n,s,i} r_i) \\ + b_{n,s}^{(i)} p_{n,s,i} K_1(\omega_{n,s,i} r_i)] \\ - \text{left} k_{22}^{(i+1)} [a_{n,s}^{(i+1)} \omega_{n,s,i+1} I_1(\omega_{n,s,i+1} r_i) \\ + b_{n,s}^{(i+1)} \omega_{n,s,i+1} K_1(\omega_{n,s,i+1} r_i)] \\ = k_{22}^{(i+1)} \frac{\partial w^{(i+1)}(r_i, n, s)}{\partial r} - k_{22}^{(i)} \frac{\partial w^{(i)}(r_i, n, s)}{\partial r} \end{aligned} \tag{32d}$$

where  $I_1$  and  $K_1$  represent modified Bessel functions of the first and second kind of order one, respectively. In order to determine series coefficients in each layer ( $a_n^{(i)}$  and  $b_n^{(i)}$ ), a set of equations consist of Eqs. (32a), (32b), (32c), and (32d) should be solved. In this set of equations, the matrix of coefficients is a five diagonal matrix. Here, the researchers used Thomas algorithm to achieve a reciprocity relations between the series coefficients in each layer:

$$a_{n,s}^{(1)} = M_{n,s}^{(1)} \tag{33a}$$

$$\begin{cases} b_{n,s}^{(i)} = N_{n,s}^{(i)} - \alpha_{n,s}^{(i)} \cdot a_{n,s}^{(i)} \\ a_{n,s}^{(i+1)} = M_{n,s}^{(i+1)} - \beta_{n,s}^{(i+1)} \cdot b_{n,s}^{(i)} \quad 1 < i < n_l - 1 \end{cases} \tag{33b}$$

$$b_{n,s}^{(n_l)} = N_{n,s}^{(n_l)} - \alpha_{n,s}^{(n_l)} \cdot a_{n,s}^{(n_l)} \tag{33c}$$

where  $\alpha_{n,s}$ ,  $\beta_{n,s}$ ,  $N_{n,s}$  and  $M_{n,s}$  for all layers are obtained from following relations:

$$\alpha_{n,s}^{(n_l)} = \frac{c_2 I_0(\omega_{n,s,n_l} r_{n_l}) + d_2 \omega_{n,s,n_l} I_1(\omega_{n,s,n_l} r_{n_l})}{c_2 K_0(\omega_{n,s,n_l} r_{n_l}) - d_2 \omega_{n,s,n_l} K_1(\omega_{n,s,n_l} r_{n_l})} \quad (34a)$$

$$N_{n,s}^{(n_l)} = \frac{G_2(n, s) - c_2 w^{(n_l)}(r_{n_l}, n, s) - d_2 \frac{\partial w^{(n_l)}(r_{n_l}, n, s)}{\partial r}}{c_2 K_0(\omega_{n,s,n_l} r_{n_l}) - d_2 \omega_{n,s,n_l} K_1(\omega_{n,s,n_l} r_{n_l})} \quad (34b)$$

$$\begin{cases} \beta_{n,s}^{(i+1)} = \frac{\pi_i}{\chi_i - \alpha_{n,s}^{(i+1)}} \\ M_{n,s}^{(i+1)} = \frac{E_i - N_{n,s}^{(i+1)}}{\chi_i - \alpha_{n,s}^{(i+1)}} \\ \alpha_{n,s}^{(i)} = \frac{\gamma_i}{\psi_i - \beta_{n,s}^{(i+1)}} \\ N_{n,s}^{(i)} = \frac{F_i - M_{n,s}^{(i+1)}}{\psi_i - \beta_{n,s}^{(i+1)}} \end{cases} \quad 1 < i < n_l - 1 \quad (34c)$$

$$M_n^{(1)} = G_1(n, s) - c_1 w^{(1)}(r_0, n, s) - d_1 \frac{\partial w^{(1)}(r_0, n, s)}{\partial r} - \frac{N_{n,s}^{(1)}(c_1 k_0(\omega_{n,s,1} r_0) - d_1 \omega_{n,s,1} K_1(\omega_{n,s,1} r_0))}{(c_1 I_0(\omega_{n,s,1} r_0) + d_1 \omega_{n,s,1} I_1(\omega_{n,s,1} r_0)) - \alpha_n^{(1)}(c_1 k_0(\omega_{n,s,1} r_0) - d_1 \omega_{n,s,1} K_1(\omega_{n,s,1} r_0))} \quad (34d)$$

where coefficients  $\pi_i$ ,  $\chi_i$ ,  $\gamma_i$ ,  $\psi_i$ ,  $E_i$  and  $F_i$  are as follows:

$$\pi_i = \frac{-I_0(\omega_{n,s,i} r_i) K_1(\omega_{n,s,i} r_i) - I_1(\omega_{n,s,i} r_i) K_0(\omega_{n,s,i} r_i)}{\frac{\omega_{n,s,i+1}}{\omega_{n,s,i}} \frac{k_{22}^{(i+1)}}{k_{22}^{(i)}} I_0(\omega_{n,s,i} r_i) K_1(\omega_{n,s,i+1} r_i) + I_1(\omega_{n,s,i} r_i) K_0(\omega_{n,s,i+1} r_i)} \quad (35a)$$

$$\chi_i = \frac{-\frac{\omega_{n,s,i+1}}{\omega_{n,s,i}} \frac{k_{22}^{(i+1)}}{k_{22}^{(i)}} I_0(\omega_{n,s,i} r_i) I_1(\omega_{n,s,i+1} r_i) + I_0(\omega_{n,s,i+1} r_i) I_1(\omega_{n,s,i} r_i)}{\frac{\omega_{n,s,i+1}}{\omega_{n,s,i}} \frac{k_{22}^{(i+1)}}{k_{22}^{(i)}} I_0(\omega_{n,s,i} r_i) K_1(\omega_{n,s,i+1} r_i) + I_1(\omega_{n,s,i} r_i) K_0(\omega_{n,s,i+1} r_i)} \quad (35b)$$

$$\gamma_i = \frac{I_0(\omega_{n,s,i} r_i)}{\chi_i \times K_0(\omega_{n,s,i+1} r_i) - I_0(\omega_{n,s,i+1} r_i)} \quad (35c)$$

$$\psi_i = \frac{\pi_i \times K_0(\omega_{n,s,i+1} r_i) + K_0(\omega_{n,s,i} r_i)}{\chi_i \times K_0(\omega_{n,s,i+1} r_i) - I_0(\omega_{n,s,i+1} r_i)} \quad (35d)$$

$$E_i = \pi_i \left[ \left( k_{22}^{(i+1)} \frac{\partial w^{(i+1)}(r_i, n, s)}{\partial r} - k_{22}^{(i)} \frac{\partial w^{(i)}(r_i, n, s)}{\partial r} \right) - \omega_{n,s,i} k_{22}^{(i)} (w^{(i+1)}(r_i, n, s) - w^{(i)}(r_i, n, s)) I_1(\omega_{n,s,i+1} r_i) \right] \quad (35e)$$

$$F_i = \frac{E_i \times K_0(\omega_{n,s,i+1} r_i) - w^{(i+1)}(r_i, n, s) - w^{(i)}(r_i, n, s)}{\chi_i \times K_0(\omega_{n,s,i+1} r_i) - I_0(\omega_{n,s,i+1} r_i)} \quad (35f)$$

The temperature distribution in frequency domain for each layer ( $\bar{\phi}^{(i)}(r, z, s)$ ) is determined by utilizing the inverse Fourier transformation (Eq. (15)) on the Eq. (29):

$$\begin{aligned} \bar{\phi}^{(i)}(r, z, s) &= \sum_{n=1}^{\infty} (U^{(i)}(r, n, s) \times \varphi_n(z)) \\ &= \sum_{n=1}^{\infty} (a_{n,s}^{(i)} I_0(\omega_{n,s,i} r) + b_{n,s}^{(i)} K_0(\omega_{n,s,i} r) + w^{(i)}(r, n, s)) \\ &\quad \times (a_1 \sin(\lambda_n z) - b_1 \lambda_n \cos(\lambda_n z)) \end{aligned} \quad (36)$$

It is important to mention that in Eq. (36), the coefficients  $a_{n,s}^{(i)}$ ,  $b_{n,s}^{(i)}$  and the arguments of Bessel functions ( $\omega_{n,s,i}$ ) are functions. The laminate temperature in time and space domain will be achieved using the inverse Laplace transformation:

$$\phi(r, z, t) = L^{-1} \{ \bar{\phi}(r, z, s) \} = \frac{1}{2\pi j} \int_{c-j\infty}^{c+j\infty} e^{st} \bar{\phi}(r, z, s) ds \quad (37)$$

where  $c$  is a constant complex number and real part of  $\bar{\phi}$ 's poles are larger than  $c$ . Finding an exact solution for complex integral expressed with Eq. (37) is very difficult or maybe impossible. Here, "Meromorphic Function method" has been used to solve this complex integral [41]. Based on this method, a function is fitted on  $\bar{\phi}$  as:

$$\bar{\phi}^{(i)}(r, z, s) = \sum_{i=1}^n \frac{\kappa_i}{s + \vartheta_i} \quad (38)$$

where  $\vartheta_i$  introduces the function poles of  $\bar{\phi}$ . Finally, the complex integral of Eq. (38) can be calculated as follows:

$$\phi^{(i)}(r, z, t) = \sum_{i=1}^n \kappa_i \exp(-\vartheta_i t) \quad (39)$$

#### 4. Results and discussion

In this section, the researchers examined the ability of the current analytical solution to solve the practical engineering problems. For this reason, we selected two applied cases consisting of a multi-layer composite coolant pipe under a longitudinally varying heat flux and a multi-layer storage tank with temperature controlled fluid. These results can be used to analyze the conductive heat transfer and thermal fracture in composite pipes and vessels. The composite material considered in this study is graphite-epoxy (25% epoxy and 75% graphite fibers). Graphite is a conductive material while epoxy is a heat insulator; as a result, there is a significant difference between conductive heat transfer coefficients indirection and perpendicular direction of fibers. This difference helps us to investigate the properties of two-dimensional orthotropic heat conduction in details. Physical properties of the fiber and matrix are presented in Table 1. The physical properties of composite which is made up of graphite and epoxy are also available in Table 2.

In order to investigate the effects of fibers' angle on temperature distribution of laminates, three different arrangements of fibers in laminate have been considered:

1. Fiber angles in all laminas are equal to zero (the fibers are winded in  $\phi$  direction) so the composite laminate is in the form of an isotropic laminate with conductive coefficients  $k_{rr} = k_{zz} = k_{22}$ .

**Table 1**  
Properties of graphite fibers and epoxy matrix [42].

Matrix material	Epoxy
Fibers material	Graphite
Conductive coefficient of matrix (W/m K)	0.19
Conductive coefficient of fibers (W/m K)	14.74
Heat capacity of matrix (J/kg K)	1613
Heat capacity of fibers (J/kg K)	709

**Table 2**  
Properties of graphite/epoxy composite material [42].

$k$ In parallel direction of fibers (W/m K)	11.1
$k$ In perpendicular direction of fibers (W/m K)	0.87
Volumetric percentage of fibers	75
Melting point (K)	450
Heat capacity (J/kg K)	935
Density (kg/m <sup>3</sup> )	1400

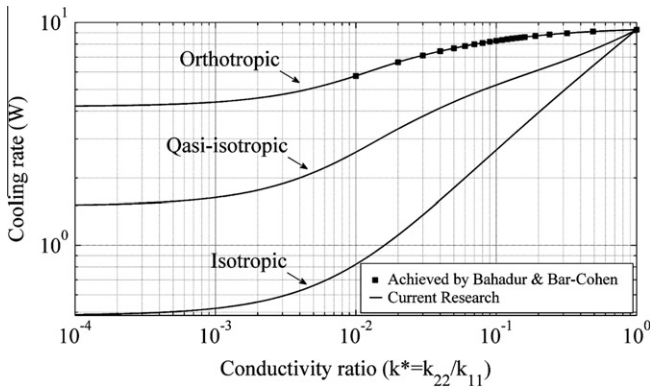


Fig. 3. Composite pin fin cooling rate variation with conductivity ratio.

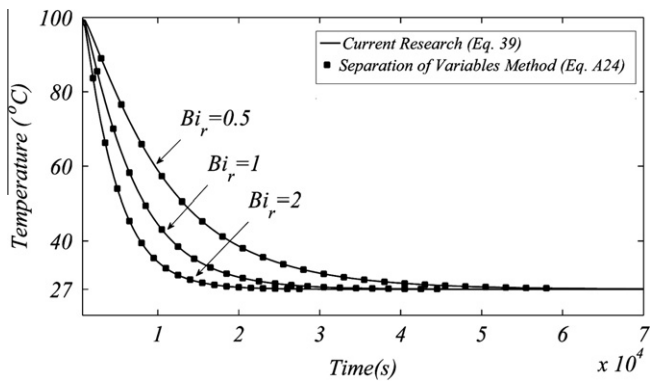


Fig. 4. History of temperature for the center of an isotropic cylinder.

2. Fiber angles in all laminas are equal to 90° (the fibers are placed in z direction) so the composite laminate is in the form of a block orthotropic material with conductive coefficients  $k_{zz} = k_{11}$  and  $k_{rr} = k_{22}$ .
3. Fibers are placed in the laminas in the form of a multi-layer quasi-isotropic laminate ( $[0^\circ, 45^\circ, 90^\circ, 135^\circ, 180^\circ, 225^\circ, 270^\circ, 315^\circ]$ ).

An analytical solution for steady heat conduction in a single layer orthotropic pin fin has been presented by Bahadur and Bar-Cohen [43]. Heat conduction in such pin fin is such a simple part of current research that the angle of fibers' in a single-layer laminate in steady state is equal to 90°. The result of Bahadur and Bar-Cohen solution is employed to validate the result of this paper. Fig. 3 shows the variation of cooling rate in terms of conductivity ratio ( $k^* = k_{11}/k_{22}$ ). This figure has been depicted in different arrangements of fibers. According to the figure, the result in

orthotropic case agrees with the result of Bahadur and Bar-Cohen [43]. Furthermore, in order to validate our results in unsteady situations, an isotropic solid cylinder under specific boundary conditions and predefined initial condition has been considered. The temperature distribution of cylinder has been achieved using separation of variables method (refer to Appendix A). The Eq. (39) should presents the same result when the fibers' angles in all laminas are equal to zero and  $k^* = 1$ . The history of temperature variation in the solid cylinder for various amount of radial Biot numbers ( $Bi_r = hr_1/K$ ) are presented in Fig. 4. The figure is depicted using both analytical solutions presented by Eqs. (39) and (A24). According to the figure, the results are completely coincident. In this study, the following applied examples are considered:

#### 4.1. Case 1: coolant pipe

Temperature distribution in a five-layer coolant pipe with longitudinally varying heat flux at outside has been considered. It is assumed that heat flux varied as a sinusoidal function,  $\dot{q}_o'' = a + b \sin(\pi z/L)$ , where  $a$  and  $b$  are two constants and  $L$  refers to length of pipe. This condition usually occurs in cooling pipe of nuclear reactors [44]. Here, we considered a five-layer graphite epoxy composite pipe and it is supposed that the reactor is cooled with air. Fig. 5 shows the geometry and boundary conditions of such a pipe. Properties of this pipe are presented in Table 3. The coefficients  $a$  and  $b$  are supposed equal to be 90 and 250  $W/m^2$ , respectively. At the left hand side of the pipe, temperature is constant and it is isolated at the other side. Moreover, there is convection inside the pipe.

#### 4.2. Case 2: storage tank

Recently, a new kind of storage tanks called “Lock-Temperature Storage Tanks” has been developed which have the ability to stratify hot and cold water. An inner chamber baffle that absorbs and eliminates turbulence caused by incoming water was used. The result is directing the hottest water to the top of the tank and the colder water to the bottom for returning to the heater. Since 1/3 less hot water storage is needed with this kind of storage tanks than with ordinary ones, so there are several economic features to consider such as, reduced water heater operation cost, lower standby losses and lower installed cost. Here, we suppose a three-layer cylindrical tank that its inside temperature varied from constant inlet temperature to outlet temperature consistent with an exponential function as  $T(z) = c + d \times \exp(z/L)$ , where  $c$  and  $d$  are related to the amount of desired outlet and inlet temperatures. If temperature changes from 300.15 to 355 K, the coefficients  $c$  and  $d$  will be 285.37 and 14.78, respectively. Convective heat transfer has been applied as the second radial boundary condition. Insulate and temperature constant conditions are also deemed for the ends of pipe. Fig. 6

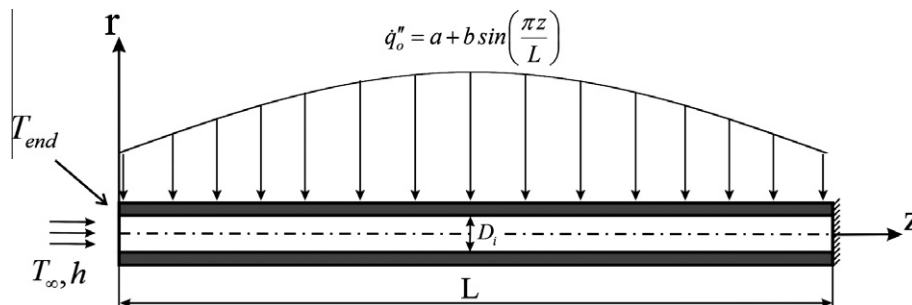


Fig. 5. Geometry and boundary conditions of cooling pipe.

**Table 3**  
Geometry and boundary conditions of cooling pipe.

Inner diameter (m)	0.25
Length (m)	3
Thickness of each layer (m)	0.015
Initial temperature (K)	373
Ambient temperature (K)	373
Internal mean temperature (K)	553
End temperature (K)	423
Convective coefficient (W/m <sup>2</sup> K)	50

shows the geometry of such tank. The geometry and boundary conditions of tank are available in Table 4.

In order to investigate the variation of temperature distribution in different arrangements of fibers, the dimensionless temperature ( $T^* = (T - T_\infty)/(T_{end} - T_\infty)$ ) is defined. Fig. 7 shows that the variation of dimensionless temperature in terms of time for three mentioned arrangements of fibers; this figure has been depicted for both cases. According to the figure, in the first and the second cases, the steady state heat conduction takes place approximately after two and twenty hours, respectively. The steady state in storage tank occurs later because compared to coolant pipe the dimension of Tank is greater. In addition, under the current boundary conditions, the amounts of mean temperature for orthotropic and isotropic laminates are maximum and minimum, respectively. It is

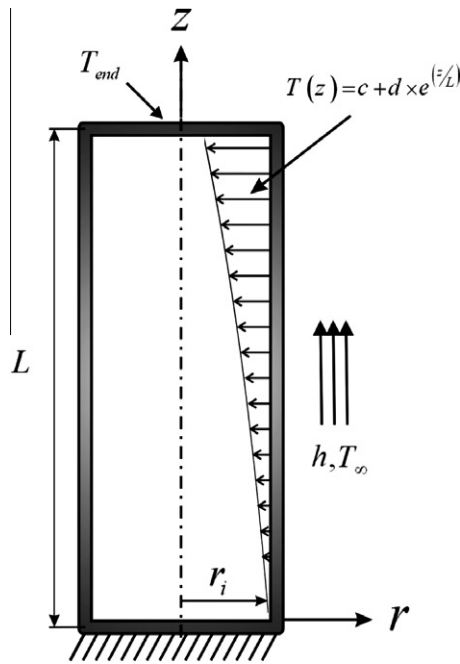


**Fig. 6.** Geometry and boundary conditions of storage tank.

**Table 4**  
Geometry and boundary conditions of storage tank.

Inner diameter (m)	0.8128
Length (m)	1.9558
Thickness of each layer (m)	0.05
Initial temperature (K)	300.15
Ambient temperature (K)	300.15
End temperature (K)	355
Convective coefficient (W/m <sup>2</sup> K)	100

consequential to mention that the heat transfer in  $r$  direction is more dominant which is related to the type of boundary conditions. When the fibers' angle approaches to 90°, the heat conduction in  $r$  direction will be decreased and the mean temperature of laminate will be increased consequently. For other arrangements of fibers, the temperature distribution is in a state between two previous states. Mean temperature history in mentioned layer arrangements are shown in Table 5. According to the Table 5, in the case of quasi-isotropic, temperature values are between the isotropic and orthotropic states.

Since two-dimensional transient heat conduction in multi-layer cylindrical laminate is studied in this paper, we should investigate the temperature distribution in radial and longitudinal direction as a function of time. Contours of temperature variation in  $r$  direction have been shown in Figs. 8 and 9 at specific longitudinal cross section for both cooling pipe and storage tank, respectively. Due to the axi-symmetric condition, radial slices of temperature contours at different times have been separated to have an obvious compare among the temperature patterns. According to the figures, temperature distributions change to reach a steady state condition by marching in time. Furthermore, these figures have been illustrated in different arrangements of fibers to present the effect of fibers' angle on temperature contours.

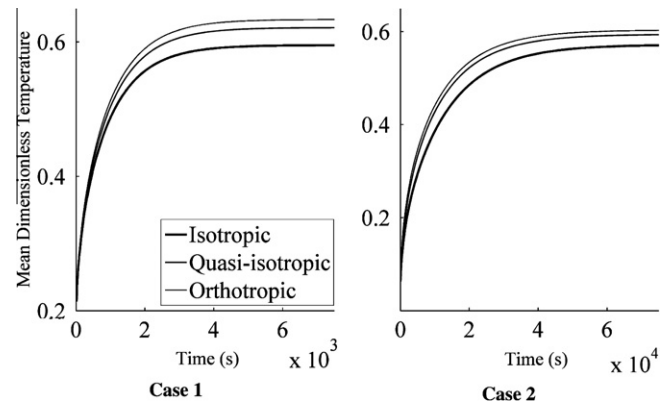


**Fig. 7.** History of temperature for cooling pipe and storage tank cases.

**Table 5**  
Mean temperature values at the various times for different arrangements of fibers.

Time (s)	Mean temperature (K)		
	Isotropic	Quasi-isotropic	Orthotropic
Case 1 15	383.6905	383.7209	383.7609
Case 2 150	304.8262	305.2026	305.5439
Case 1 100	386.8671	387.0110	387.1684
Case 2 1000	308.3813	309.3789	310.0306
Case 1 200	389.3152	389.5764	389.8151
Case 2 2000	311.2415	312.6955	313.4415
Case 1 400	392.2634	392.6966	393.0198
Case 2 4000	314.7791	316.6960	317.4708
Case 1 1000	397.2854	398.0841	398.5427
Case 2 10000	321.2276	323.5080	324.2480
Case 1 1500	399.5293	400.5196	401.0399
Case 2 15000	324.5615	326.7461	327.4423
Case 1 2500	401.5884	402.7711	403.3478
Case 2 25000	328.2335	330.0773	330.6973
Case 1 3500	402.3383	403.5967	404.1931
Case 2 35000	329.9728	331.5479	332.1170
Case 1 5000	402.6638	403.9567	404.5611
Case 2 50000	331.0077	332.3691	332.8995
Case 1 7500	402.7454	404.0473	404.6534
Case 2 75000	331.4271	332.6769	333.1871

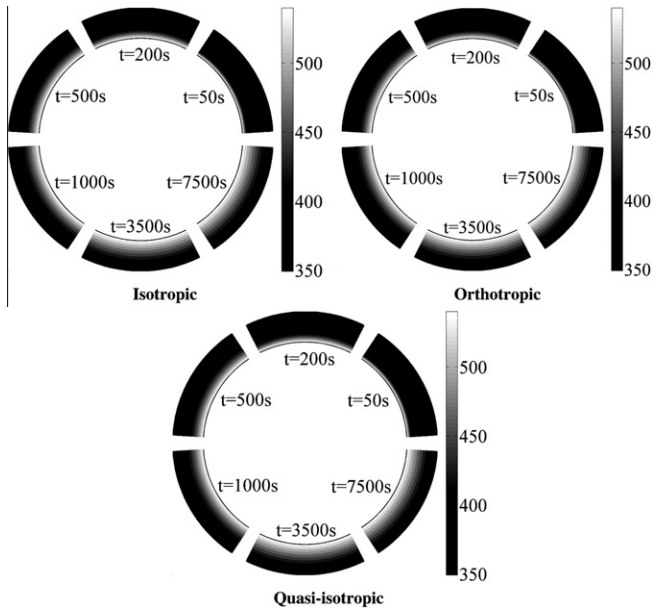


Fig. 8. Contours of temperature distribution in radial direction in section  $z = L/2$  at the different times for cooling pipe case.

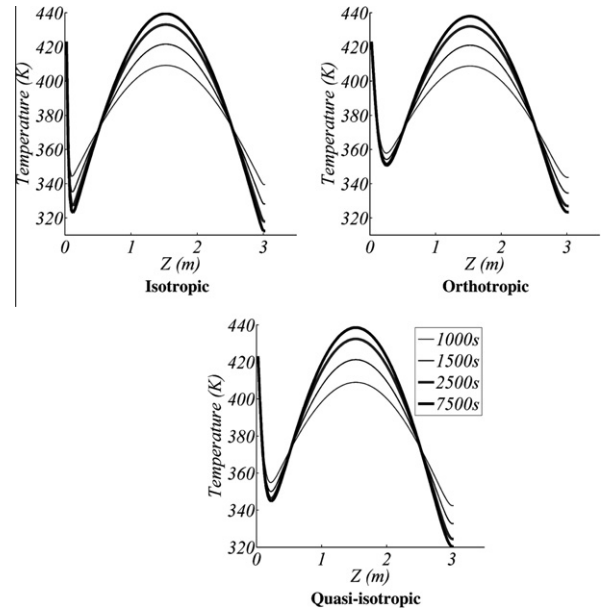


Fig. 10. Temperature distribution in longitudinal direction in section  $r = R + \text{thickness}/2$  at the different times for cooling pipe case.

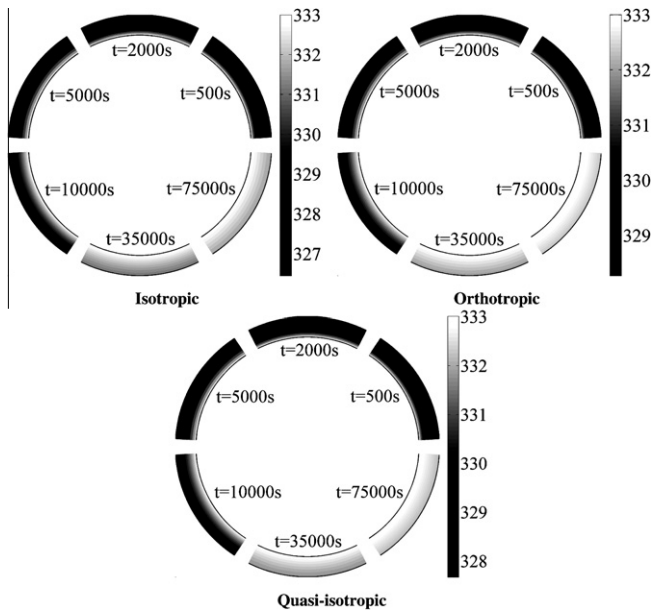


Fig. 9. Contours of temperature distribution in radial direction in section  $z = L/2$  at the different times for storage tank case.

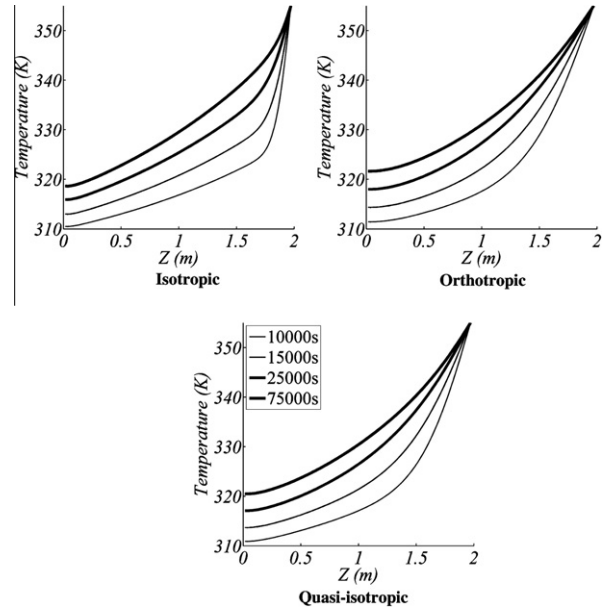


Fig. 11. Temperature distribution in longitudinal direction in section  $r = R + \text{thickness}/2$  at the different times for storage tank case.

Figs. 10 and 11 show variation of temperature distributions in  $z$  direction versus time at the specific radial section for cases 1 and 2, respectively. Here, the temperature distributions in this direction are mainly affected with longitudinal boundary conditions outside the cooling pipe and inside the storage tank, respectively. In the first case, a symmetric sinusoidal boundary condition in  $z$  direction has been applied and as it is seen in Fig. 10, a maximum temperature will be located at the middle longitudinal section of pipe. In the second case, an exponential function has been considered for boundary condition inside of storage tank. For this kind of boundary conditions, temperature increases from minimum value at the bottom to its maximum at the top of tank according to an exponential function in all laminates.

### 5. Conclusion

In the current research, an analytical solution for transient heat conduction in multi-layer composite laminates has been presented. This solution is obtained for generalized linear thermal boundary conditions and can be used for various types of applied situations without any assumption. The results that are obtained in this investigation can be employed for predicting and controlling the thermal stress and thermal fraction in composite structures. When the angle of fibers is zero, temperature gradient is least and heat conduction is more effective in fibers. In contrast, when the angle of fibers in laminas increases, mean temperature of laminates will increase in such a form that the most temperature

amount occurs at  $\theta = 90^\circ$ . Regarding to the thermal designing objectives, the appropriate selection of composite material and fibers' arrangement in each lamina must be implemented to have desired heat conduction through the laminate. This method introduced in previous sections can be used for any cylindrical multi-layered laminates such as composite reservoirs, heat exchangers, pipes, pin fins and so on.

**Appendix A. Analytical solution for heat conduction in an isotropic medium**

Unsteady heat conduction equation in radial and longitudinal dimension for an isotropic medium is as follow:

$$\frac{\partial^2 T}{\partial r^2} + \frac{1}{r} \frac{\partial T}{\partial r} + \frac{\partial^2 T}{\partial z^2} = \frac{1}{\alpha} \frac{\partial T}{\partial t} \tag{A1}$$

In order to achieve an exact solution for this equation, we consider a rod of radius  $r_1$  under the following boundary and initial conditions which enable us to solve it with separation of variables method as an alternative exact method.

$$T(r, 0, t) = T_\infty \tag{A2a}$$

$$\frac{\partial T(r, L, t)}{\partial z} = 0 \tag{A2b}$$

$$T(0, z, t) = \text{finite} \tag{A2c}$$

$$-k \frac{\partial T(r_1, z, t)}{\partial r} = h(T(r_1, z, t) - T_\infty) \tag{A2d}$$

$$T(r, z, 0) = T_i \tag{A2e}$$

For the first step, we must homogenize the boundary conditions in both  $r$  and  $z$  directions. Here, the modified temperature has been defined as follows:

$$\phi(r, z, t) = T(r, z, t) - T_\infty \tag{A3}$$

Using this modified temperature, the formulation of problem will change to:

$$\frac{\partial^2 \phi}{\partial r^2} + \frac{1}{r} \frac{\partial \phi}{\partial r} + \frac{\partial^2 \phi}{\partial z^2} = \frac{1}{\alpha} \frac{\partial \phi}{\partial t} \tag{A4}$$

subjected that

$$\phi(r, 0, t) = 0 \tag{A5a}$$

$$\frac{\partial \phi(r, L, t)}{\partial z} = 0 \tag{A5b}$$

$$\phi(0, z, t) = \text{finite} \tag{A5c}$$

$$-k \frac{\partial \phi(r_1, z, t)}{\partial r} = h\phi(r_1, z, t) \tag{A5d}$$

$$\phi(r, z, 0) = \phi_i(z) = (T_i - T_\infty) \tag{A5e}$$

Using the product solution  $\phi(r, z, t) = R(r)Z(z)T(t)$ , we can separate the differential Eq. (A4) in the following form:

$$\frac{1}{R(r)} \left( \frac{\partial^2 R(r)}{\partial r^2} + \frac{1}{r} \frac{\partial R(r)}{\partial r} \right) + \frac{1}{Z(z)} \frac{\partial^2 Z(z)}{\partial z^2} = \frac{1}{\alpha T(t)} \frac{\partial T(t)}{\partial t} = -\lambda^2 \tag{A6}$$

which leads in the following equation for time function ( $T(t)$ ):

$$\frac{\partial T(t)}{\partial t} + \alpha \lambda^2 T(t) = 0 \tag{A7}$$

Furthermore, by rearranging the first equality of Eq. (A6) in the following form, we have

$$\frac{1}{R(r)} \left( \frac{\partial^2 R(r)}{\partial r^2} + \frac{1}{r} \frac{\partial R(r)}{\partial r} \right) + \lambda^2 = \frac{-1}{Z(z)} \frac{\partial^2 Z(z)}{\partial z^2} = \mu^2 \tag{A8}$$

Therefore, the following differential equation and boundary conditions are obtained in  $z$  direction:

$$\frac{\partial^2 Z(z)}{\partial z^2} + \mu^2 Z(z) = 0; \quad Z(0) = 0, \quad \frac{\partial Z(L)}{\partial z} = 0 \tag{A9}$$

The second characteristic differential equation and boundary conditions in  $r$  direction are as follows:

$$\frac{\partial^2 R(r)}{\partial r^2} + \frac{1}{r} \frac{\partial R(r)}{\partial r} + \kappa^2 R(r) = 0; \quad R(0) = \text{finite}, \quad -kR'(r_1) = hR(r_1) \tag{A10}$$

where  $\kappa^2 = \lambda^2 + \mu^2$ . The solution of Eq. (A9) is

$$Z_n(z) = A_n \varphi_n(x), \quad \varphi_n(x) = \sin \mu_n z \tag{A11}$$

where the characteristic values are  $\mu_n = (2n - 1)\pi/2L, n = 1, 2, 3, \dots$ . The solution of Eq. (A10) gives

$$R_m(r) = B_m \psi_m(r), \quad \psi_m(r) = J_0(\kappa_m r) \tag{A12}$$

where the characteristic values,  $\kappa_m$ , are the zeros of  $J'_0(\kappa_m r_1) + (h/k)J_0(\kappa_m r_1) = 0$  and,  $J_0$  represent the Bessel functions of the first kind, of order zero. The solution of Eq. (A7) is

$$T_{nm}(t) = C_{nm} e^{-\alpha \lambda_{nm}^2 t}; \quad \lambda_{nm}^2 = \mu_n^2 + \kappa_m^2 \tag{A13}$$

Hence, the product solution becomes

$$\phi(r, z, t) = \sum_{n=1}^{\infty} \sum_{m=1}^{\infty} a_{nm} e^{-\alpha \lambda_{nm}^2 t} \times J_0(\kappa_m r) \times \sin(\mu_n z) \tag{A14}$$

where  $a_{nm} = A_n B_m C_{nm}$ . The non-separable initial condition (Eq. (A5e)) gives

$$\phi_i(z) = \sum_{n=1}^{\infty} \left( \sum_{m=1}^{\infty} a_{nm} J_0(\kappa_m r) \right) \times \sin(\mu_n z) \tag{A15}$$

Using the relation of Fourier–Bessel series [40,45], the coefficient of this series can be calculated. The interior summation can be considered as the coefficient of Fourier sine series and calculated as

$$\sum_{m=1}^{\infty} a_{nm} J_0(\kappa_m r) = \frac{2}{L} \int_0^L \phi_i(z) \sin(\mu_n z) dz = \phi_{in} \tag{A16}$$

where

$$\phi_{in} = \frac{2}{\mu_n L} [(T_i - T_\infty)] \tag{A17}$$

Using the relation of Bessel functions [45], we have

$$a_{mn} = \frac{\int_0^{r_1} r \phi_{in} J_0(\kappa_m r) dr}{\int_0^{r_1} r J_0^2(\kappa_m r) dr} \tag{A18}$$

where the  $\kappa_m$  is a root of  $J'_0(\kappa_m r_1) + (h/k)J_0(\kappa_m r_1) = 0$ , the denominator of Eq. (A18) is

$$\int_0^{r_1} r J_0^2(\kappa_m r) dr = \frac{(\kappa_m^2 + (h/k)^2) r_1^2}{2\kappa_m^2} J_0^2(\kappa_m r_1) \tag{A19}$$

The numerator of Eq. (A18) equals

$$\int_0^{r_1} r \theta_{in} J_0(\kappa_m r) dr = \frac{r_1 \phi_{in}}{\kappa_m} J_1(\kappa_m r_1) \tag{A20}$$

Substituting Eqs. (A19) and (A20) into the Eq. (A18), yields:

$$a_{mn} = \frac{2\phi_{in}(\kappa_m r_1) J_1(\kappa_m r_1)}{[\kappa_m^2 r_1^2 + Bi_r^2] J_0^2(\kappa_m r_1)}, \quad Bi_r = \frac{hr_1}{k} \tag{A21}$$

where  $J_1$  represent the Bessel functions of the first kind, of order one. This relation may further be rearranged by considering the outer boundary condition ( $J_0'(\kappa_m r_1) + (h/k)J_0(\kappa_m r_1) = 0$ ) which is equivalent to

$$\kappa_m r_1 J_1(\kappa_m r_1) = Bi_r J_0(\kappa_m r_1) \quad (A22)$$

Substituting Eq. (A22) into Eq. (A21), we have

$$a_{nm} = \frac{2\phi_{in} Bi_r}{[\kappa_m^2 r_1^2 + Bi_r^2] J_0(\kappa_m r_1)} \quad (A23)$$

Finally, introducing the Eq. (A23) into Eqs. (A14) and (A3), we find the solution as

$$T(r, z, t) = T_\infty + \sum_{n=1}^{\infty} \sum_{m=1}^{\infty} \frac{2\phi_{in} Bi_r}{[\kappa_m^2 r_1^2 + Bi_r^2] J_0(\kappa_m r_1)} e^{-\alpha_m^2 t} J_0(\kappa_m r) \times \sin(\mu_n z) \quad (A24)$$

## References

- [1] W. Krenkel, F. Berndt, C/C–SiC composites for space applications and advanced friction systems, *Mater. Sci. Eng., A* 412 (2005) 177–181.
- [2] J. Jedidi, F. Jacquemin, A. Vautrin, Design of accelerated hygrothermal cycles on polymer matrix composites in the case of a supersonic aircraft, *Compos. Struct.* 68 (2005) 429–437.
- [3] C.J. von Klemperer, D. Maharaj, Composite electromagnetic interference shielding materials for aerospace applications, *Compos. Struct.* 91 (2009) 467–472.
- [4] P. Filip, Z. Weiss, D. Rafaja, On friction layer formation in polymer matrix composite materials for brake applications, *Wear* 252 (2002) 189–198.
- [5] Z. Stadler, K. Krnel, T. Kosmac, Friction and wear of sintered metallic brake linings on a C/C–SiC composite brake disc, *Wear* 265 (2008) 278–285.
- [6] Y. Xia, A.M. Jacobi, An exact solution to steady heat conduction in a two-dimensional slab on a one-dimensional fin: Application to frosted heat exchangers, *Int. J. Heat Mass Transfer* 47 (2004) 3317–3326.
- [7] X. Fang, Z. Zhang, Z. Chen, Study on preparation of montmorillonite-based composite phase change materials and their applications in thermal storage building materials, *Energy Convers. Manage.* 49 (2008) 718–723.
- [8] S. Pashah, A.F.M. Arif, Syed M. Zubair, Study of orthotropic pin fin performance through axisymmetric thermal non-dimensional finite element, *Appl. Therm. Eng.* 31 (2011) 376–384.
- [9] M.T. Mustafa, Syed M. Zubair, A.F.M. Arif, Thermal analysis of orthotropic annular fins with contact resistance: A closed-form analytical solution, *Appl. Therm. Eng.* 31 (2011) 937–945.
- [10] L.A. Dobrzanski, M. Drak, B. Ziebowicz, New possibilities of composite materials application—Materials of specific magnetic properties, *J. Mater. Process. Technol.* 191 (2007) 352–355.
- [11] R. Olivé-Monllau, M.J. Esplandiú, J. Bartrolí, M. Baeza, F. Céspedes, Strategies for the optimization of carbon nanotube/polymer ratio in composite materials: Applications as voltammetric sensors, *Sensors Actuat. B* 146 (2010) 353–360.
- [12] K. Fujihara, K. Teo, R. Gopal, P.L. Loh, V.K. Ganesh, S. Ramakrishna, K.W.C. Foong, C.L. Chew, Fibrous composite materials in dentistry and orthopaedics: Review and applications, *Compos. Sci. Technol.* 64 (2004) 775–788.
- [13] E. Stodolak, T. Gumula, R. Leszczynski, J. Wiczorek, S. Blazewicz, A composite material used as a membrane for ophthalmology applications, *Compos. Sci. Technol.* 70 (2010) 1915–1919.
- [14] J.R. Xiao, D.F. Gilhooley, R.C. Batra, J.W. Gillespie Jr., M.A. McCarthy, Analysis of thick composite laminates using a higher-order shear and normal deformable plate theory (HOSNDPT) and a meshless method, *Compos. B* 39 (2008) 414–427.
- [15] D.A. Papargyris, R.J. Day, A. Nesbitt, D. Bakavos, Comparison of the mechanical and physical properties of a carbon fiber epoxy composite manufactured by resin transfer molding using conventional and microwave heating, *Compos. Sci. Technol.* 68 (2008) 1854–1861.
- [16] U. Topal, U. Uzman, Thermal buckling load optimization of laminated composite plates, *Thin Walled Struct.* 46 (2008) 667–675.
- [17] H. Bakaiyan, H. Hosseini, E. Ameri, Analysis of multi-layered filament-wound composite pipes under combined internal pressure and thermo mechanical loading with thermal variations, *Compos. Struct.* 88 (2009) 532–541.
- [18] V. Antonucci, M. Giordano, K.T. Hsiao, S.G. Advani, A methodology to reduce thermal gradients due to the exothermic reactions in composites processing, *Int. J. Heat Mass Transfer* 45 (2002) 1675–1684.
- [19] Z.S. Guo, S. Du, B. Zhang, Temperature field of thick thermoset composite laminates during cure process, *Compos. Sci. Technol.* 65 (2005) 517–523.
- [20] T. Behzad, M. Sain, Finite element modeling of polymer curing in natural fiber reinforced composites, *Compos. Sci. Technol.* 67 (2007) 1666–1673.
- [21] I. Dlouhy, Z. Chlup, D.N. Boccaccini, S. Atiq, A.R. Boccaccini, Fracture behaviour of hybrid glass matrix composites: Thermal ageing effects, *Compos. A* 34 (2003) 1177–1185.
- [22] A. Gilbert, K. Kokini, S. Sankarasubramanian, Thermal fracture of zirconia–mullite composite thermal barrier coatings under thermal shock: An experimental study, *Surf. Coat. Technol.* 202 (2008) 2152–2161.
- [23] A. Gilbert, K. Kokini, S. Sankarasubramanian, Thermal fracture of zirconia–mullite composite thermal barrier coatings under thermal shock: A numerical study, *Surf. Coat. Technol.* 203 (2008) 91–98.
- [24] M. Blanc, M. Touratier, A constrained discrete layer model for heat conduction in laminated composites, *Comput. Struct.* 83 (2005) 1705–1718.
- [25] M. Kaminski, Homogenization-based finite element analysis of unidirectional composites by classical and multiresolutional techniques, *Comput. Methods Appl. Mech. Eng.* 194 (2005) 2147–2173.
- [26] C. Corlay, S.G. Advani, Temperature distribution in a thin composite plate exposed to a concentrated heat source, *Int. J. Heat Mass Transfer* 50 (2007) 2883–2894.
- [27] S.E. Lee, J.S. Yoo, J.H. Kang, C.G. Kim, Prediction of the thermal conductivities of four-axial non-woven composites, *Compos. Struct.* 89 (2009) 262–269.
- [28] J. Schuster, D. Heider, K. Sharp, M. Glowania, Thermal conductivities of three-dimensionally woven fabric composites, *Compos. Sci. Technol.* 68 (2008) 2085–2091.
- [29] D. Bhattacharjee, V.K. Kothari, Heat transfer through woven textiles, *Int. J. Heat Mass Transfer* 52 (2009) 2155–2160.
- [30] M.H. Hsieh, C.C. Ma, Analytical investigations for heat conduction problems in anisotropic thin-layer media with embedded heat sources, *Int. J. Heat Mass Transfer* 45 (2002) 4117–4132.
- [31] C.C. Ma, S.W. Chang, Analytical exact solutions of heat conduction problems for anisotropic multi-layered media, *Int. J. Heat Mass Transfer* 47 (2004) 1643–1655.
- [32] S. Singh, P.K. Jain, Rizwan-uddin, Analytical solution to transient heat conduction in polar coordinates with multiple layers in radial direction, *Int. J. Therm. Sci.* 47 (2008) 261–273.
- [33] M.H. Kayhani, M. Shariati, M. Norouzi, M.K. Demneh, Exact solution of conductive heat transfer in cylindrical composite laminate, *Heat Mass Transfer* 46 (2009) 83–94.
- [34] M.H. Kayhani, M. Norouzi, A. Amiri Delouei, A general analytical solution for heat conduction in cylindrical multilayer composite laminates, *Int. J. Therm. Sci.* 52 (2012) 73–82.
- [35] M.N. Ozisik, *Heat Conduction*, second ed., Wiley, New York, 1993.
- [36] Y.C. Fung, *Foundation of Solid Mechanics*, Prentice-Hall, Englewood Cliffs, 1965.
- [37] J.M. Powers, On the necessity of positive semi-definite conductivity and on sager reciprocity in modeling heat conduction in anisotropic media, *J. Heat Transfer Trans. Asme* 126 (5) (2004) 670–675.
- [38] C.T. Herakovich, *Mechanics of Fibrous Composites*, Wiley, New York, 1998.
- [39] J.C. Halpin, *Primer on Composite Materials Analysis*, CRC Press, Boca Raton, 1992.
- [40] T. Myint-U, L. Debnath, *Linear Partial Differential Equations for Scientists and Engineers*, Birkhauser, Boston, 2007.
- [41] I.N. Bronshtein, K.A. Semendyayev, G. Musiol, H. Muehlig, *Hand Book of Mathematic*, Springer, 1998.
- [42] Y.S. Touloukian, C.Y. Ho, *Thermophysical properties of matter, Thermal Conductivity of Nonmetallic Solids*, vol. 2, Plenum press, New York, 1972.
- [43] R. Bahadur, A. Bar-Cohen, Orthotropic thermal conductivity effect on cylindrical pin fin heat transfer, *Int. J. Heat Mass Transfer* 50 (2007) 1155–1162.
- [44] W.M. Kays, M.E. Crawford, B. Weigand, *Convective Heat and Mass Transfer*, 4th ed., McGraw-Hill, New York, 2005.
- [45] V.S. Arpaci, *Conduction Heat Transfer*, Addison-Wesley, Massachusetts, 1996.